Detection of Radio Emission from Air Showers in the MHz Range at the Pierre Auger Observatory

Jens Neuser* for the Pierre Auger Collaboration†

*Bergische Universität Wuppertal, Germany
†Pierre Auger Observatory, Av. San Martín Norte 304, 5613 Malargüe, Argentina
(Full author list: `http://www.auger.org/archive/authors_2014_08.html`)

Abstract. The Auger Engineering Radio Array (AERA) at the Pierre Auger Observatory in Argentina has been constructed in multiple stages starting in 2010. The current stage consists of 124 dual-polarized radio detector stations covering an area of 6 km^2. One of the main goals is to study the radio emission processes for energies beyond 10^{17} eV in the range from 30 to 80 MHz. Having the unique opportunity for multi-hybrid measurements of air showers in combination with the surface detector, the fluorescence detector and also the low-energy extensions at the Pierre Auger Observatory, AERA is a milestone for further large-scale radio experiments. Combining the advantages of other detector types, AERA is investigating the sensitivity to air shower parameters.

This paper gives an overview of the motivation and science goals of AERA and shows the current status and performance of the detector. First multi-hybrid events will be presented as well as the most recent results. Polarization measurements, which show a strong evidence for a contribution of a radial polarized emission component in the air showers, will be discussed. An outlook with future perspectives will be given.

Keywords: cosmic rays, extensive air showers, Pierre Auger Observatory, AERA, radio detection, MHz
PACS: 07.57.-c, 95.55.Vj, 96.50sd

1. INTRODUCTION

The detection of radio emission from extensive air showers has been under theoretical and experimental study for about 50 years. Although already predicted by Askaryan [1] and measured by Jelley et al. [2] in the 1960s, only 10 years ago new detector experiments like LOPES [3] and CODALEMA [4] have led to a renaissance of the radio detection technique showing that the reconstruction of air shower properties is possible using modern technologies. Thereby, a radio detector (RD) combines several advantages of other detector types making it a promising candidate for further large-scale air shower experiments. On the one hand the radio technique is sensitive to the longitudinal shower development like a fluorescence detector, which can be used to determine the composition of the primary cosmic rays. On the other hand the detector can be operated with almost 100% duty cycle. Moreover the detecting element itself, the antenna, is a very simple and therefore cost effective entity, which still yields a very good angular resolution.

Based within the bounds of the Pierre Auger Observatory the AERA experiment is sited in a perfect environment for tests and calibration of improved methods for determining air shower properties with the radio technique at the highest energies. Combining the precise knowledge of the antenna gain and electronic characteristics, including a calibration of the entire signal chain, with an incoming shower direction enables the reconstruction of the electric field vector at the radio detector station (RDS). Therefore, AERA is capable of performing hybrid-analyses like energy estimation or composition studies in combination with other Pierre Auger Observatory detectors as well as stand-alone radio-analyses to investigate the radio emission process, for example by polarization studies.

2. THE PIERRE AUGER OBSERVATORY AND AERA

The Pierre Auger Observatory is constructed in the rural environment of the Pampa Amarilla in the province of Mendoza in Argentina. The observatory consists of over 1600 autonomous water-Cherenkov particle detectors (SD) arranged in a 1.5 km grid covering an area of about 3000 km^2, which are overlooked by 24 fluorescence telescopes (FD) located at four different sites around the array (see Fig. 1). The deployment of those baseline detectors was

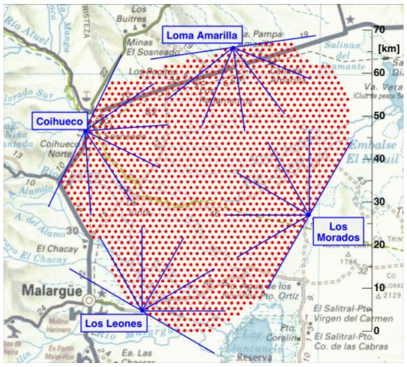

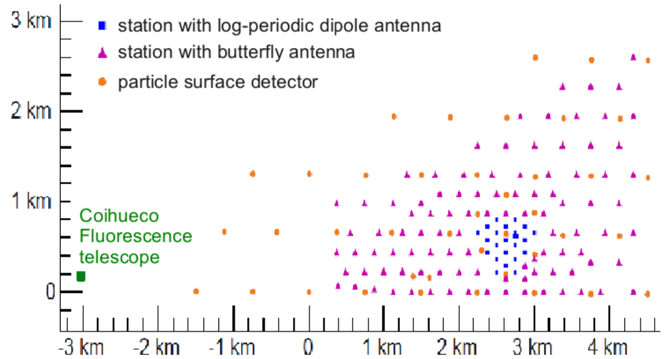

FIGURE 1. Map of the Pierre Auger Observatory in Argentina. SD stations are shown with red circles, the fields of view of the FD telescopes are indicated by blue lines.

FIGURE 2. Layout of the Auger Engineering Radio Array in front of Coihueco. AERA-24 stations are marked with blue squares, AERA-124 stations by purple triangles. The nearby SD-Infill stations are shown with orange circles.

completed in 2008 and since then, the two components have been providing high-quality hybrid measurements of ultra-high-energy cosmic rays. Additionally, low-energy extensions have been built up in the last years [5, 6]. The AMIGA detector adds 60 more SD stations to the ground array, which are deployed in a 750 m grid (the so-called *infill*), as well as additional muon detectors (MD) for some of these stations. The HEAT enhancement includes three more fluorescence telescopes at the FD site Coihueco which can observe showers with a higher elevation angle. These detectors are of special interest for AERA as they are both co-located with the radio array.

AERA is the radio extension of the Pierre Auger Observatory and located inside the Infill as well as in the field of view of the FD site Coihueco. It is constructed in three different deployment stages with the final goal of a > 15 km^2 detector array filled with $\sim$ 160 RDS. It is and will be used to address the following objectives:

- Measure the radio emission from air showers and describe the underlying *emission process(es)* in the frequency range from 30 - 80 MHz above 10^{17} eV,
- Measure the *composition* in the energy range of the transition region from galactic to extragalactic origin of cosmic rays,
- Explore the general *feasability of radio measurements* with stand-alone radio detectors or in combination with the Auger baseline detectors and enhancements as well as for further large-scale experiments.

The first stage, AERA-24, has been deployed in 2010 after successful tests of several small prototype setups and reached stable operation in March 2011. Twenty-four RDS equipped with a dual-polarized log-periodic dipole antenna (LPDA) [7] were placed on 0.5 km^2 with a spacing of 150 m (see Fig. 2). A solar powered read-out chain with low-noise amplifier, digitizer and GPS allowed fully autonomous operation except for a fiber connection to the central DAQ. A major step was achieved in April 2011, when the first coincidences with SD could be measured. In April 2013 100 additional RDS were deployed now covering an area of about 6 km^2 with spacings of 250 / 375 m forming AERA-124. Besides updated digital front-end electronics also a different physical antenna, the Butterfly [7, 8], was used for the new RDS and the communcication with the DAQ is now realized using a WiFi system. To explore several trigger possibilities complementary to the self-triggering, one part of the RDS is able to be externally triggered (e.g. by the other Auger detectors) while the other part is equipped with additional scintillators. For further information about the technological developments for AERA see [9].

3. DATA PROCESSING AND RECONSTRUCTION

After the event data have been processed by the central DAQ the binary files are stored on a local RAID system. This results in a data volume ($\sim$ 40 GB/day) which can not be transfered to Europe for further processing directly. Therefore, a dedicated radio server was set up in Argentina to host several production steps. First of all, the binary data are converted into streams for different purposes, as for instance physical analyses and monitoring. Then, the events from the physical analysis stream are merged into a combined set with data from the other Auger detectors. This enables

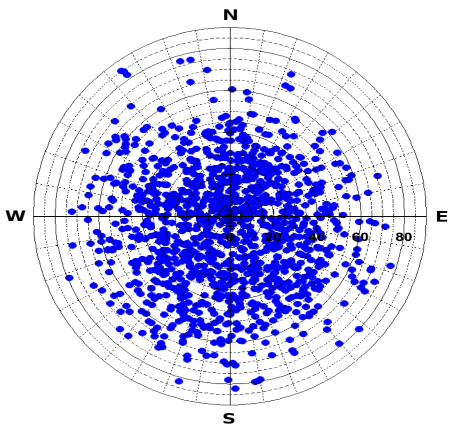

FIGURE 3. Skymap of the radio reconstructed cosmic ray arrival directions for the SD-externally triggered AERA events from October 2013 to March 2014.

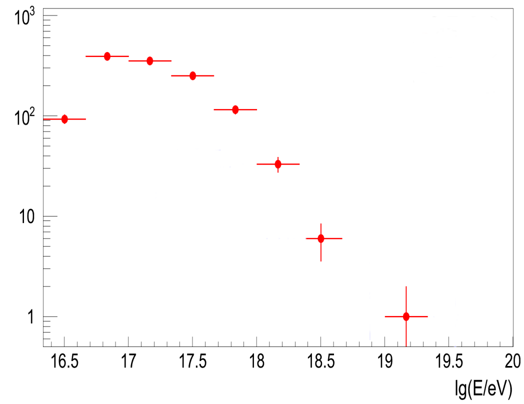

FIGURE 4. Reconstructed energy for the SD events in coincidence with AERA based on the data from the SD Infill from October 2013 to March 2014.

the possibility for an immediate hybrid-reconstruction using the Auger-$\overline{\text{Off}}\underline{\text{line}}$ analysis framework [10] which for the moment includes SD-Infill, FD-HEAT and AERA data. To deal with the different and varying detector components mentioned in Sec. 2, the full time-dependent detector description has been implemented using a database. This includes especially all analog components to allow a full unfolding of the detector response. Afterwards, successfully reconstructed events are selected and stored in the merged low-level format as well as in an advanced format for high-level analysis and transferred to a central storage place of Auger.

Using these files one can easily get an overview on some fundamental air shower properties. Fig. 3 shows a skyplot of the reconstructed arrival directions for radio events in coincidence with SD in a period from October 2013 to March 2014. The result reflects two separate effects: A *north-south assymmetry* due to the geomagnetic emission (see Sec. 4.1) and a *loss of sensitivity towards the horizon* coming from the antenna gain pattern as well as the SD trigger efficiency. Fig. 4 shows the energy distribution of the primary cosmic rays determined using the SD-Infill data for the same set of events. The maximum at 10^{17} eV corresponds to the full trigger efficiency threshold for the infill array.

In Fig. 5 an example of an event triggered by SD is shown. Around four-five of these coincidences are measured per day. Although only four RDS had a signal above a signal-to-noise cut the directional reconstruction is found to be in good agreement with the direction obtained from SD and FD.

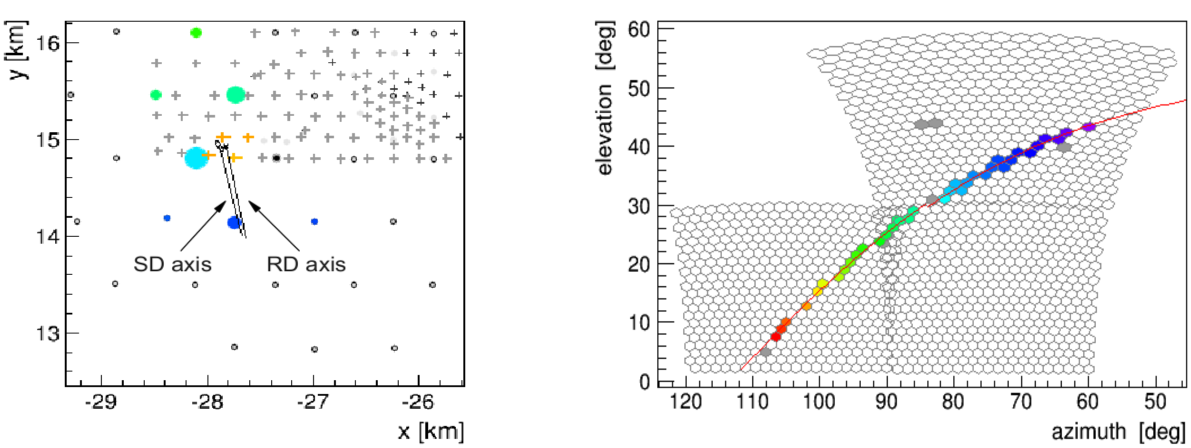

FIGURE 5. Example of a *super-hybrid* event as reconstructed with $\overline{\text{Off}}\underline{\text{line}}$. The left plot shows the SD stations (circles) as well as the AERA stations (crosses). The shower axes, reconstructed by RD and SD respectively, are displayed with the solid lines, color coding indicates the signal arrival time. The coincident measurement of FD & HEAT is shown in the right plot.

4. PHYSICS RESULTS

4.1. Radio Emission Process and Polarization

One of the major physics objectives of AERA is the investigation of the radio emission process of air showers. The geomagnetic contribution was first predicted in 1967 by Kahn & Lerche [11] and was confirmed to be the dominant process in the MHz regime by LOPES [12] and CODALEMA [13, 14]. The charged shower particles are deflected by the Lorentz force while traveling through the geomagnetic field in the atmosphere. This effect induces a time-varying transverse current which then causes the coherent radio emission. Therefore, to first order, the radio signal is polarized in the direction of the Lorentz vector $\mathbf{v} \times \mathbf{B}$ ($\mathbf{v}$: direction of the shower axis, $\mathbf{B}$: direction of the geomagnetic field at the detection site). This also leads to the excess of radio events measured with AERA coming from the south (see Fig. 3). Additionally, another effect was proposed by Askaryan already in 1962 [1]. The annihilation of positrons and knock-out electrons from air molecules in the shower leads to a time-varying net charge excess resulting in a radially polarized electric field. Therefore, it is possible to disentangle the two different components through the different polarization angles in the associated electric field.

This analysis has been done with data from AERA-24 by comparing the polarization angle measured at the RDS with predictions based on a model of the two components. For further information on the underlying calculations see [15]. The measured angle is calculated using the Stokes parameters, which can be directly calculated from a complex representation of the electric field vector for the different polarizations. The theoretical model assumes a contribution with a radial polarization in addition to the geomagnetic process. The parameter a gives the relative strength of the electric fields induced by the charge-excess (E^A) and by the geomagnetic (E^G) emission process taking into account the geomagnetic angle α:

$$a \equiv sin(\alpha)\frac{|E^A|}{|E^G|} \tag{1}$$

The result of the comparison assuming a pure geomagnetic emission, i.e. $a = 0$, is shown on the left side of Fig. 6. A clear correlation between measured and predicted polarization angles can be seen resulting in a Pearson correlation coefficient of $\rho_p = 0.82^{+0.06}_{-0.04}$ at 95% C.L. for this dataset. Calculating the reduced χ^2 yields a value of χ^2/ndf = 27.

Using the equation for the theoretical model it is possible to calculate a for each individual measurement by varying it over a wide range and to obtain a most probable value. The result of this scan is displayed in Fig. 7. One can clearly see that the values of a_i do not arise from a single constant value of a, which might be due to the fact that those values depend on more parameters (e.g. zenith angle). For this data-set a mean value of $\overline{a} = 0.14 \pm 0.02$ has been determined.

This mean value now can be used to re-evaluate the predicted polarization angle also including the deduced uncertainties. The result is shown on the right side of Fig. 6 yielding a significantly increased correlation with a Pearson correlation coefficient of $\rho_p = 0.93^{+0.04}_{-0.03}$ at 95% C.L. This improvement is also reflected in a χ^2/ndf = 2.2.

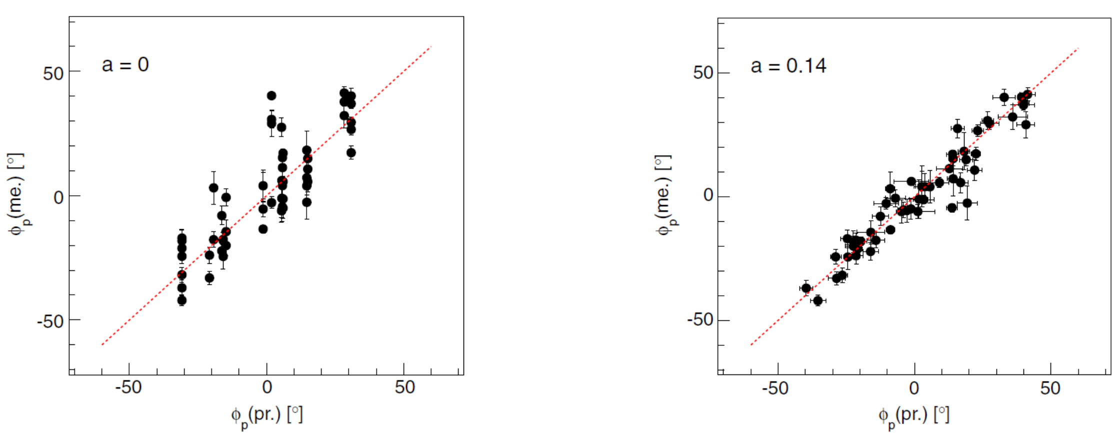

FIGURE 6. Predicted polarization angle assuming a pure geomagnetic emission with $a = 0$ (left) and a combination of two emission mechanisms with $a = 0.14$ (right) versus the measured polarization angle for the AERA-24 data set [15].

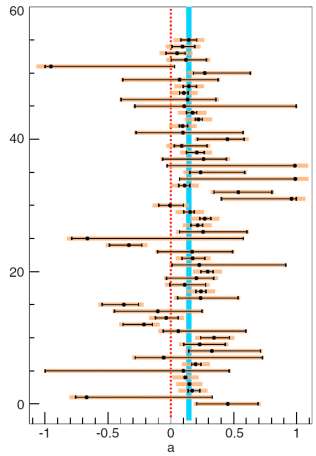

FIGURE 7. Distribution of the most probable values of a and their uncertainties per event. The mean value of a is indicated with the solid blue line [15].

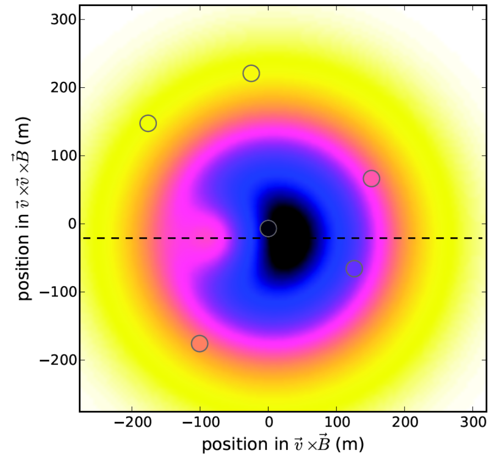

FIGURE 8. Example event for a fitted two-dimension lateral distribution function. Colored contour represents the fitted, colored circles the measured signal.

Therefore, we can state that a clear evidence for a radial component in the radio emission process has been measured with a strength of $(14\pm2)\%$ compared to the geomagnetic component. This result is supported by the analysis of data obtained with one of the AERA prototype setups as well as some older results from different experiments [16, 17].

4.2. Lateral distribution function and further analysis topics

An adequate knowledge of the lateral distribution function of the radio signal is crucial for many further high-level analyses. Therefore, several attempts have been made to find an appropriate description, but it turned out that neither a simple one- or two-dimensional exponential approach motivated from earlier observations [18] yields a sufficient approximation to the observed distributions. This can easily be understood with the interference of the two emission-mechanisms described in Sec. 4.1. Using a phenomenological approach one finds a two-dimensional double gaussian as promising candidate:

$$P(x',y') = A_+ \cdot exp\left(\frac{-|(x'-X_+)^2+(y'-Y_+)^2|}{\sigma_+^2}\right) - A_- \cdot exp\left(\frac{-|(x'-X_-)^2+(y')^2|}{\sigma_-^2}\right) \tag{2}$$

With this superposition it is possible to describe the two main features of the radio signal. The exponential fall-off further away from the core with the A_+-term and the dip due to the Cherenkov-compression enhanced ring around the core with the A_--term. Additionally, the displacement of the Gauss-centers can model the interference of the two polarized emission mechanisms. Fig. 8 shows an example event. Before applying the two-dimensional fit, the signal positions are transformed into the $\mathbf{v}\times\mathbf{B}$ and $\mathbf{v}\times\mathbf{v}\times\mathbf{B}$ plane of the shower. The colored contour shows the fit result whereas the colored circles represent the signal of the individual stations. One can clearly see that fit and measurement are in good agreement. This function has first been applied to LOFAR data [19]. It has been successfully tested on some first AERA events and is under further investigation.

Additional analyses concerning an energy estimator for radio, the composition determination using $X_{\max}$ and signal studies like risetime are currently ongoing [20].

5. FUTURE PLANS

Simulation studies have shown that there is a significantly higher efficiency for the radio detection of *inclined* air showers. While the radial detection limit for a shower with zenith angle of $\theta = 30^\circ$ only reaches distances up to hundreds of meters from the shower core, it goes up to 2 kilometers or more for a shower with $\theta = 75^\circ$ (see also [21]). Detecting those showers will require an accurate measurement of the vertically polarized shower component which for the current dual-polarized antennas can only be calculated using the two horizontal components under the assumption of the propagation-direction of the transverse wave. Therefore, AERA is testing several prototypes for a three-dimensional antenna. These stations have been deployed inside the AERA field in November 2013 and are taking first data. Also an antenna prototype for low frequency measurements has been installed at the same time.

The deployment of 25 additional RDS is planned for the next year. Although not yet finally decided one idea would be to install these detectors in close vicinity to the existing SD stations to be able to perform an individual measurement of the electromagnetic shower component at the same location.

6. CONCLUSION

AERA is built up as the radio extension of the Pierre Auger Observatory since 2010 and yields the unique opportunity for *super-hybrid* shower detection in combination with the other detectors of the observatory. The deployment of 124 radio detector stations on $\sim$ 6 km^2 has successfully been completed in May 2013. An automated data and reconstruction pipeline has been established to provide input for high-level analyses on a short delay time. Using the data from AERA-24 a 14% contribution of an Askaryan-like radial polarized component was found. A two-dimensional lateral distribution function with a double-gaussian approach has been tested successfully on first events. Further analyses on major physics objectives are currently ongoing. Additional radio detector stations will be deployed in the near future which may include also the possibility of three-dimensional and/or low frequency measurements of radio emission. Also the feasibility of measurements of different shower components at the same location is under investigation. The excellent data of the Pierre Auger Observatory allows one to test the capabilities of the radio-detection for various shower quantities towards a precise measurement of the incoming cosmic ray.

REFERENCES

1. G. A. Askaryan, *Soviet Physics JETP* **14**, 441 (1962).
2. J. V. Jelley, et al., *Nature* **205**, 327-328 (1965).
3. H. Falcke, et al., Nature (London) **435**, 313 (2005).
4. D. Ardouin, et al., Astropart. Phys. **26**, 341 (2006).
5. H. J. Mathes, et al. (for the Pierre Auger Coll.), "The HEAT Telescopes of the Pierre Auger Observatory: Status and First Data" in *Proc. of the 32nd ICRC, Beijing, China* (2011), `arXiv:1107.4807`.
6. F. Sanchez, et al. (for the Pierre Auger Coll.), "The AMIGA detector of the Pierre Auger Observatory: an overview" in *Proc. of the 32nd ICRC, Beijing, China* (2011), `arXiv:1107.4807`.
7. P. Abreu, et al. (for the Pierre Auger Coll.), J. Instrum. **7**, P10011 (2012).
8. D. Charrier (for the CODALEMA Coll.), in *Proc. of the ARENA 2010 workshop (Nantes, France)*, Nucl. Instr. and Meth. **A662**, S142, `http://dx.doi.org/10.1016/j.nima.2010.10.141`.
9. J. Maller (for the Pierre Auger Coll.), "Technological developments for the Auger Engineering Radio Array" in *Proc. of the ARENA 2014 workshop (Annapolis, USA)*, AIP Conference Proceedings, to be published.
10. P. Abreu, et al. (for the Pierre Auger Coll.), *Nucl. Instrum. Meth.* **A635**, 92-102 (2011).
11. F. D. Kahn and I. Lerche, "Radiation from Cosmic Ray Air Showers" in *Royal Society of London Proc. Series A* **289**, 206-213 (1966).
12. A. Horneffer, W. D. Apel, J. D. Arteaga, et al., "Primary Particle Energy Calibration of the EAS Radio Pulse Height" in *International Cosmic Ray Conference*, 2008, vol. 4 of *International Cosmic Ray Conference*, pp. 83-86.
13. D. Ardouin, et al., *Astropart.Phys.* **31**, 192-200 (2009), `arXiv:0901.4502`.
14. B. Revenu, "Evidence for a geomagnetic effect in the CODALEMA radio data" in *Proc. of the 31st ICRC, Lodz, Poland*, 2009, `arXiv:0906.2832`.
15. A. Aab, et al. (for the Pierre Auger Coll.), *Phys. Rev. D* **89**, 052002 (2014).
16. J. H. Hough and J. D. Prescott, in *Proc. of the VI Interamerican Seminar on Cosmic Rays* (Universidad Mayor de San Andres, La Paz, Bolivia, 1970), Vol. 2, p.527.
17. J. R. Prescott, J. H. Hough, and J. K. Pidcock, Nature (London) Phys. Sci. **233**, 109 (1971).
18. H. R. Allan, in *Progress in Particle and Nuclear Physics: Cosmic Ray Physics* (North-Holland Publishing Company, Amsterdam, 1971), Vol. 10, p. 169.
19. A. Nelles, et al., "A parameterization for the radio emission of air showers as predicted by CoREAS simulations and applied to LOFAR measurements", *Astropart. Phys.* **60**, 13-24 (2014), `arXiv:1402.2872`.
20. Q. Dorosti Hasankiadeh (for the Pierre Auger Coll.), "Advanced Reconstruction Strategies for the Auger Engineering Radio Array" in *Proc. of the ARENA 2014 workshop (Annapolis, USA)*, AIP Conference Proceedings, to be published.
21. O. Kambeitz (for the Pierre Auger Coll.), "Radio Detection of Horizontal Extensive Air Showers with AERA" in *Proc. of the ARENA 2014 workshop (Annapolis, USA)*, AIP Conference Proceedings, to be published.